Accelerated growth of oxide film on aluminium alloys under steam: Part II: Effects of alloy chemistry and steam vapour pressure on corrosion and adhesion performance

Din, Rameez Ud; Bordo, Kirill; Jellesen, Morten Stendahl; Ambat, Rajan

Published in:
Surface and Coatings Technology

Link to article, DOI:
10.1016/j.surfcoat.2015.06.060

Publication date:
2015

Document Version
Peer reviewed version

Accelerated growth of oxide film on aluminium alloys under steam: Part II: Effects of alloy chemistry and steam vapour pressure on corrosion and adhesion performance

Rameez Ud Din, Kirill Bordo, Morten S. Jellesen, Rajan Ambat

PII: S0257-8972(15)30097-9
DOI: doi: 10.1016/j.surfcoat.2015.06.060
Reference: SCT 20359

To appear in: *Surface & Coatings Technology*

Received date: 29 October 2014
Revised date: 16 June 2015
Accepted date: 25 June 2015

Please cite this article as: Rameez Ud Din, Kirill Bordo, Morten S. Jellesen, Rajan Ambat, Accelerated growth of oxide film on aluminium alloys under steam: Part II: Effects of alloy chemistry and steam vapour pressure on corrosion and adhesion performance, *Surface & Coatings Technology* (2015), doi: 10.1016/j.surfcoat.2015.06.060

Accelerated growth of oxide film on aluminium alloys under steam: Part II: Effects of alloy chemistry and steam vapour pressure on corrosion and adhesion performance

Rameez Ud Din[1], Kirill Bordo, Morten S. Jellesen, Rajan Ambat

Department of Mechanical Engineering, Technical University of Denmark, Kongens Lyngby 2800, Denmark

Abstract

The steam treatment of aluminium alloys with varying vapour pressure of steam resulted in the growth of aluminium oxyhydroxide films of thickness range between 450 - 825 nm. The surface composition, corrosion resistance, and adhesion of the produced films was characterised by XPS, potentiodynamic polarization, acetic acid salt spray, filiform corrosion test, and tape test. The oxide films formed by steam treatment showed good corrosion resistance in NaCl solution by significantly reducing anodic and cathodic activities. The pitting potential of the surface treated with steam was a function of the vapour pressure of the steam. The accelerated corrosion and adhesion tests on steam generated oxide films with commercial powder coating verified that the performance of the oxide coating is highly dependent on the vapour pressure of the steam.

Keywords: Steam, vapour pressure, aluminium alloys, corrosion, acetic acid salt spray, filiform corrosion

[1] Corresponding author e-mail:rudin@mek.dtu.dk

1 Introduction

Aluminium and its alloys are widely used in construction, automotive and aerospace industry because of their distinct properties, for instance light weight, low toxicity and valuable corrosion resistance characteristics [1,2]. Heat-treatable 6000 series aluminium alloys are heavily used in automotive and construction industry owing to fuel efficiency, weight reduction, formability and strength [3,4]. The native oxide film of about 2-10 nm thick on an aluminium alloy, is stable in natural environments in the absence of chloride and provides natural corrosion resistance to the metal. Nonetheless the native oxide film has inadequate barrier properties for long term corrosion prevention of the underlying metal substrate, even after being further coated by organic protective coatings [5]. Therefore an intermediate layer of conversion coating is needed. Function of conversion coatings is to improve the corrosion resistance and build a base for subsequent application of organic coatings with improved adhesion [6]. An organic coating alone is permeable to water and other ions over long periods of time due to the micro-pores and diffusion through the molecular structure [7].

Although banned today due to carcinogenic issues [8], chromate-based conversion treatment [9] is the most protective conversion coating due to the re-passivation provided by the self-healing ability of chromate. A number of alternative conversion coatings are in use, however none of them have been proven to be as good as chromate-based conversion treatments. Alternative surface treatment techniques applied to aluminium alloys include Ti/Zr based conversion coatings, which are commercially available and include polymeric constituents. These coatings are applied by dipping or spraying to generate a 10-50 nm thick oxide film [10,11]. However the corrosion performance of these coatings has been shown to be inferior when compared to the chromate-based conversion coating treatment [12]. Other alternatives for chromate based conversion coating treatments include rare earth based inhibitors [13], organic polymer coatings [14], and phosphating process [15] with some

additives for aluminium alloys [16]. These processes have some drawbacks, like e. g. polymers are difficult to work with unless used with chromates and use of rare earth inhibitors add to the cost. Phosphate based coatings individually or with addition of chromates provide good paint adhesion, but corrosion resistance is inferior to that of chromate-based conversion treatments [17]. Earlier studies [18–20] reported that steam based conversion coatings exhibit good corrosion resistance properties by reducing anodic and cathodic activities of aluminium.

The interaction of applied top coat with metal substrate is determined by the chemical and physical nature of pre-treated aluminium alloy surface. The adhesion provided by the mechanical interlocking is one aspect which depends on the surface morphology of the conversion coating [21,22]. The adhesion mechanism also depends on the acid/base properties of the surface due to the possibility of forming chemical bonds with the top layer [23]. The organic molecules in the top layer will form chemical bonds with the conversion layer depending on the surface property. The presence of hydroxyl group is an important aspect due to the possibility of forming bonds by donating negatively charged oxygen [24]. Rider [25] reported that adhesion and durability of applied epoxy coating was affected by boiling water treatment of aluminium. Strålin and Hjertberg [26] found that the adhesion of ethylene vinyl acetate polymer with a pseudo-boehmite aluminium oxyhydroxide layer is stronger than with a dehydroxylated aluminium oxide.

In the present investigation aluminium alloy surfaces are treated with steam to generate relatively thick oxide layers. Part I of this paper describes in detail, the microstructure, surface morphology, oxide growth mechanism and phase analysis of the steam generated oxide films as a function of steam parameters. This paper (Part II) studies surface chemistry and electrochemical behaviour of steam generated oxide films evaluated on Peraluman 706™ and AA1090. The acid salt spray, filiform corrosion resistance, and adhesion properties of the oxide films were examined according to relevant standards, and therefore using AA6060 alloy

[27]. Moreover the adhesion properties of these oxide films were judged in dry and wet conditions by tape test. The oxide films were produced at different vapour pressures of steam and compared for the surface chemistry and corrosion performance.

2 Experimental

2.1 Materials

The elemental composition of the aluminium alloys Peraluman 706™ and AA1090 was presented in Part I. The alloys were in the form of cold rolled sheets with the thickness of 1 mm and 0.5 mm respectively. All samples were cut from the sheet into 50 x 50 mm coupons. The commercial AA6060 aluminium alloy was used for industrial scale corrosion performance testing. The alloy specimens were cut from 1 mm thick sheet into 150 x 50 mm coupons. The alloy chemical composition obtained from the supplier data sheet is presented in table I.

2.2 Surface preparation

2.2.1 Treatment 1

All samples were degreased by dipping in 6 wt. % commercial Alficlean (pH=9) aqueous solution for 2 minutes at 60 °C followed by rinsing in deionized water for 1 minute and air drying at room temperature.

2.2.2 Treatment 2

Samples were subjected to alkaline etching treatment by immersing in an aqueous solution of 10 wt. % NaOH at 60 °C for 5 minutes, rinsing in deionized water for 1 minute followed by desmutting in 69 % vol. HNO_3 for 2 minutes. The specimens were then washed with deionized water and dried in air at room temperature.

2.3 Steam Treatment

Samples from treatment 1 and treatment 2 were exposed to steam treatment in an autoclave. The surfaces of the specimens were exposed to 5 psi, 10 psi, and 15 psi (gauge pressure) pressurized steam which was generated from deionized water in an autoclave (All American Pressure Canners, USA). The total process time was 25 minutes, while the time of exposure after the autoclave reached steady state conditions was 10 minutes. The maximum temperature measured by THERMAX (TMC,UK) surface indicator strips, at 5 psi, 10 psi, and 15 psi internal pressure in the autoclave was 107 °C, 113 °C, and 118 °C respectively. The vapour pressure of the steam was calculated in bar by using Antoine equation.

$$\ln P^{\circ} = -B/T+C + A \qquad [28]$$

Where P is vapour pressure, B, C, and A are the component-specific constants for Antoine equation and T is the temperature at which vapours are generated.

2.4 Oxide coating surface analysis

2.4.1 X-ray photoelectron spectroscopy (XPS)

The XPS analysis was performed using a Thermo Scientific K-Alpha X-ray photoelectron spectrometer equipped with an Al Kα (1486.6 eV) X-ray source. Survey spectra were measured in the range from 0 to 1100 eV with pass energy of 200 eV. High-resolution spectra for the Al 2*p* and O 1*s* levels were measured with pass energy of 50 eV; 10 scans were performed in each case. Binding energies were measured with a precision of ± 0.1 eV. Surface charge compensation was performed using a low energy electron flood gun. All binding energies were referenced to the C 1*s* line at 285.0 eV. Photoelectrons were collected at 90° with respect to the sample surface. The analysed area had a diameter of 400 µm. The base pressure in the analysis chamber was approximately $2x10^{-8}$ mbar. The deconvolution of the XPS spectra for the Al 2*p* and O 1*s* levels was made by commercial peak fitting software (XPSPeak 4.1).

2.5 Corrosion performance

2.5.1 Electrochemical behaviour

Potentiodynamic polarization measurements were carried out using an ACM electrochemical Instrument (GillAC). A flat cell set-up with an exposed area of 0.95 cm^2 was used for measurements. The open circuit potential (OCP) was monitored for 15 min prior to conducting the polarization scans. The anodic and cathodic sweeps were conducted separately in naturally aerated 0.1M NaCl solution. An Ag/AgCl reference electrode and a Pt wire counter electrode were employed. All polarization scans were conducted at a scan rate of 1 mV/s starting from a potential close to OCP. All experiments were repeated two times for consistency on two different samples.

2.5.2 Acetic acid salt spray (AASS)

The acetic acid salt spray (AASS) DIN EN ISO 9227 standard test was carried out on selected samples of AA6060 aluminium alloy treated with different vapour pressure of the steam. The AA6060 alloy specimens having size 150 mm x 50 mm x 1 mm were powder coated after the surface treatment. The specimens were powder coated with a conventional polyester coating type Jotun Facade 2487 RAL 9010 and cured at 170 ºC for 30 min by achieving final thickness of 80-90 µm. For AASS two replica samples of each treatment have been tested.

2.5.3 Filiform corrosion (FFC)

The AA6060 alloy test coupons, 150 mm x 50 mm x 1 mm in size were steam treated at various steam pressures. The specimens after surface treatment were powder coated with Jotun Facade 2487 RAL 9010 having final thickness within 80-90 µm after curing at 170 ºC for 30 min. The filiform corrosion (FFC) tests and final evaluation of the tested sample was conducted according to DIN EN 3665, corresponding to the standard FFC test conditions. For FFC two replica samples of each treatment have been tested.

2.6 Adhesion testing

Tape adhesion measurements were carried out on powder coated specimens which involve scratching four parallel lines with a diamond knife down to the metal substrate, vertically and horizontally with a separation of approximately 1 mm followed by applying a tape over the scratched area and pulling it up with a steady force at 90º. After the tape test, the areas with scratched lines were exposed to AASS for 1000 hours and the tape tests were performed again on the same scratched area.

3 Results

3.1 Presence of hydroxyl groups at the surface

The near-surface chemical composition of the steam treated surfaces of AA1090 samples was analysed using XPS with an aim of understanding the specific structure of oxide and surface functional groups. Figure 1 (a), (b) shows XPS spectra of the Al 2*p* level for the samples obtained after 30 s and 10 min of steam treatment, respectively. The binding energy of the Al 2*p* peak after taking the surface charging into account was found to be about 74.1 eV which is a characteristic of Al in oxidation state +3 [29]. Since the chemical shifts of the Al 2*p* level are very similar for Al_2O_3 and boehmite [30,31], it is not possible to distinguish between the two species based on the Al 2*p* spectra. However, it was shown previously [30,32–36] that the individual contributions from these species could be obtained by deconvolution of the O 1*s* line. In Figure 1 (c) and Figure 1 (d) the XPS spectra of the O 1*s* level for the samples obtained after 30 s and 10 min of steam treatment are presented. The spectra were fit by 3 Gaussian-Lorenzian peaks, assuming the presence of 3 oxygen-containing species in the analysed films: O^{2-} in the structure of boehmite or Al_2O_3, OH^- in boehmite, and adsorbed water H_2O_{ads}. With increase in the process time, the intensity of the O^{2-} component increases, while the intensities of the OH^- and H_2O_{ads} components remain

almost constant. The full width at half maximum (FWHM) of the OH^- peak decreases from 2.1 eV for 30 s of steam treatment to 1.8 eV for 10 min.

3.2 Electrochemical behaviour

The potentiodynamic cathodic and anodic polarization curves of Peraluman 706™ samples after treatment 1 and treatment 2 followed by steam treatment for 10 min at different vapour pressures are shown in Figure 2 and Figure 3, respectively. The cathodic polarization curves presented in Figure 2 (a) and 3 (a) show that the steam treatment has significant effect on cathodic behaviour by lowering the current densities by 2 orders of magnitude, while the change in vapour pressure from 1.3 to 1.9 bar did not generate any additional effect.

The anodic polarization curves presented in Figure 2 (b) and 3 (b) show almost a four orders of magnitude decrease in current densities for the steam treated surface, while the passive current density values remain essentially similar for all vapour pressures. The etched (treatment 2) and non-etched (treatment 1) surfaces showed significant difference, exhibiting higher breakdown potential for etched sample compared to non-etched samples. The increase in the vapour pressure of the steam also resulted in more stable oxide film at higher potential values, shown by the increased breakdown potential. Polarization curve for 1.3 bar vapour pressure showed lowest breakdown potential with sudden increase in current, while increased vapour pressure has resisted the breakdown of the oxide film. Table II shows the breakdown potential of oxide film of the steam treated samples at different vapour pressure at which the pitting occurred.

For comparison, anodic and cathodic current densities for all polarization curves corresponding to -480 mV and -1100 mV are presented in Figure 4. Results indicate that the pre-treatment of the alloy has an effect on anodic activity. Anodic current densities of steam treated samples of AA1090 and Peraluman 706™ increases initially for increase of vapour pressure from 1.3 bar to 1.6 bar, while it decreases for 1.9 bar pressure. The scatter plot revealed that the pre-treatment of the alloy plays a vital role in anodic activity at lower vapour

pressure of steam, but samples treated at high vapour pressure of steam did not show a similar effect of pre-treatment. However, the measured anodic current densities for the steam treated samples decreased after pre-treatment 2 for both alloys.

The steam treatment of Peraluman 706™ leads to higher cathodic activity as compared to AA1090. However, the measured cathodic current densities of the steam treated samples (treatment 1, treatment 2) of both alloys at different vapour pressures were very close to each other.

The SEM images in Figure 5 show the morphology of the anodic attack in 0.1M NaCl solution of pH 5.3±0.3 during polarization. Very few pits were found at the surface of steam treated samples (Figure 5 (c)) in comparison with the reference aluminium sample (Figure 5 (a)). The observed pit morphology inside the pit in all cases was crystallographic in nature. Figure 5 (b) and Figure 5 (d) show high magnification images of undissolved crystallographic planes. This form of attack was similar for all alloys after steam treatment at different vapour pressure of steam.

3.3 Standardised corrosion testing

The AA6060 contains similar alloying elements as in Peraluman 706™ (Mg-Si alloys), however the amount of these alloying elements varies between both the alloys. The microstructural features in both alloys are also quite similar i.e. Al-Fe-Si based intermetallic particles. Moreover, the purpose of using AA6060 for filiform corrosion and acetic acid salt spray testing was to compare the quality standard of steam-based conversion coatings to that of chromate based and other standardised chrome free conversion coatings. Certain standards are in use across different industries according to the demand and usage of different aluminium alloys [27,37]. Hence, according to standard [27], acetic acid salt spray test and filiform corrosion test have been performed on AA6060 which is an Al-Mg-Si alloy. On the basis of electrochemical data, the entire test samples were pre-treated by treatment 2 followed by steam treatment for 10 min at 1.3, 1.6, and 1.9 bar vapour pressure of steam, respectively

3.3.1 Acetic acid salt spray (AASS)

Accelerated AASS tests are typically used to determine if the coating on substrates have enough field exposure performance. In this test, oxide coatings generated by steam at 1.3, 1.6, and 1.9 bar vapour pressure have been compared. According to DIN EN ISO 9227 standards, tests have been carried out on steam treated powder coated samples for 1000 hours. Figure 6 shows the surface of powder coated samples after exposure to acetic acid salt spray test where the corrosion attack has been observed. Majority of the samples showed the area next to the scratch was fairly intact, while few places showed under creep corrosion. Further, the penetration depth of the corrosion attack was higher for steam treated samples at 1.3 bar of vapour pressure in contrast to 1.6 and 1.9 bar steam treated samples. The average maximum length of corrosion attack for samples treated with various vapour pressure of steam is shown in Figure 7. It shows that the increase in vapour pressure of steam resulted in lower corrosion attack. However, vapour pressure of steam at 1.6 and 1.9 bar showed identical performance. Furthermore, the reference sample showed the highest degree of delamination.

3.3.2 Filiform corrosion

The morphology of a typical FFC filament on steam treated powder coated samples after 1000 hours of FFC is shown in figure 8. It is evident that the FFC filaments initiate perpendicular to the applied scratch and the typical width of the filament was in the range of 300-500 µm in all cases. Further, the direction of the filament was arbitrary after growth of few microns. The number of filaments per length of scratch on all the samples exhibited a minor variation, although the filament density in case of the sample treated with 1.3 bar vapour pressure of steam was slightly higher in comparison to the sample treated at 1.9 bar. The overall corrosion results, assessed by the length of FFC filament perpendicular to the scratch are reported in Figure 9.

The maximum corrosion attack on the samples from the applied longitudinal and horizontal scratch is indicated by coloured bars horizontal line pattern, while the minimum length of corrosion attack is represented by box pattern coloured bars. The threshold of 2 mm length for FFC filament is frequently used to distinguish between acceptable and unacceptable filiform corrosion resistance of the coating. Overall the length of FFC attack on all the steam treated samples was below this threshold frequency. However, there was significant difference between the lengths of FFC filaments on the samples.

As shown in figure 9, the sample treated with 1.9 bar of vapour pressure of steam exhibited a relatively high corrosion resistance in comparison to all the samples which were treated at lower vapour pressure of steam, i.e. 1.3 bar, 1.6 bar. Further, the sample treated with 1.9 bar of vapour pressure of steam also displayed lowest values of FFC filament length in the longitudinal and horizontal direction. In general, lengths of FFC attack in the extrusion direction of AA6060 decreased by the increase in the vapour pressure of steam. The entire set of samples did not show any blistering of paint at the rest of the areas where no FFC attack was observed. The reference sample showed intensive delamination of powder coating i.e. > 8 mm.

3.4 Adhesion

3.4.1 Adhesion of powder coating prior to AASS and after

The tape adhesion tests were performed on the samples instantly after the curing of powder coating by making a cross cut. During the tape test no failed region was observed in all samples.

The cross cut samples were then exposed to 1000 hours of AASS. After the AASS exposure, the squares inside the grid were investigated with optical microscope and tape test was repeated on the same areas.

Figure 10 shows individual square in the grid after the AASS test, where "P" represents intact powder coating and "C" represents the areas of detached powder coating. The detachment of the powder coating on the sample treated at 1.3 bar vapour pressure of steam was intensive (marked by C). However the samples treated at 1.6 and 1.9 bar of vapour pressure of steam showed the corrosion attack which was restricted to the edges of square in the grid.

Figure 11 shows the hatch area after the tape test on the samples exposed to AASS for 1000 hours. It is evident that the delamination of powder coating took place for 1.3 bar steam treatment. Further, the samples treated at 1.6 and 1.9 bar of vapour pressure of steam showed the lift out of powder coating at the edges, while majority of the powder coating was still intact with the steam generated oxide films.

4 Discussion

The present study showed that the steam generated oxide films produced on aluminium alloys were corrosion resistant and provided adequate adhesion between the powder coating and metal substrate. Further, the performance of the coating was improved by the use of high vapour pressure of steam together with an industrially applied powder coating system. The effect of steam treatment on the microstructure of the alloys used in the present study and chemical composition of formed oxide films have been reported in our previous studies [18,38]. It has been described that the increase in the vapour pressure of steam resulted in the formation of oxide films of distinct surface morphologies, compactness, thickness, and coverage of intermetallic particles. The reported results clearly show that the oxide formed on aluminium alloys under the steam conditions were boehmite. However, the crystallinity of the oxide was dependent on the time of the steam treatment. Shorter steam treatment time for aluminium alloys resulted in less amount of crystalline boehmite films. The formation of boehmite is also confirmed by XPS results (O 1*s* peak fit). The width (FWHM) of the OH^-

peak decreases from 2.1 eV for 30 s of steam treatment to 1.8 eV for 10 min. Thus XPS results are in an agreement with the GI-XRD data [38] for the same samples and indicate an increased degree of crystallinity in the films obtained after a longer time of steam treatment. Notably, XPS analysis indicates presence of hydroxyl groups at the oxide surface which plays a vital role in the adhesion of polymer to the hydrated aluminium oxide surface [39,40]. Moreover, the XPS measurements were accompanied by strong surface charging, which resulted in a significant shift of the spectra towards the higher binding energies. This effect is typical for XPS measurements on poorly conductive samples and it makes any quantitative comparison of the obtained data rather problematic. Therefore the amounts of hydroxyl groups on the surface for different samples were only qualitatively compared.

Potentiodynamic polarization shows that the steam generated oxide film increases the corrosion resistance of the alloy. The iron containing intermetallic particles act as noble sites in aluminium matrix [41]. The corrosion potential of aluminium substrate after steam treatment shifted towards negative values in comparison to non-treated surface. As iron containing intermetallic particles shifts the corrosion potential of aluminium alloys to nobler side, the coverage of these cathodic intermetallic particles by the formed oxide film may shift the corrosion potential to negative side. Pitting potential is significantly affected by the increased steam pressure in the treatment, and it is assumed to be due to the compactness of the oxide film at high vapour pressure [38]. Pre-treatment 1 followed by pressurised steam treatment showed inferior corrosion resistance as compared to pre-treatment 2, which can be related to the removal of some intermetallic phases and the better coverage of intermetallic particles at high vapour pressure of steam [38]. The presence of different intermetallic phases in aluminium matrix makes the surface prone to localised corrosion [42–44]. Hence the coverage of intermetallic particles with the oxide film results in the enhancement of corrosion resistance of the aluminium alloys.

For powder coated aluminium, FFC takes place where defects are present [45]. The FFC testing of steam generated oxide films with increased vapour pressure exhibited behaviour similar to the polarization measurements. The length and density of filiform corrosion filaments decrease by the increase in the vapour pressure of the steam. This phenomenon can be directly attributed to the change in the microstructure of the alloy after steam treatment. It was observed that the steam treatment of AA1090 and Peraluman 706™ at lower vapour pressure of steam resulted in poor coverage of intermetallic particles and lower thickness of oxide film over aluminium matrix [38]. Potentiodynamic polarization data obtained on AA1090 and Peraluman 706™ showed that the pitting potential was shifted towards nobler side after steam treatment with high vapour pressure of steam (1.9 bar), was in good agreement with the industrial standardised FFC test results of AA6060.

Standardised AASS is used to study the detachment of powder coating with the steam generated oxide films at various vapour pressures of steam. In general, a high degree of detachment of the powder coating was observed on the samples treated with lower vapour pressure of steam. The steam treatment of AA1090 and Peraluman 706™ at lower vapour pressure of steam resulted in less compact morphology of the oxide film [38]. This explains that the oxide film generated at lower provides permeable membrane which yields in high degree of migration of chloride ions/electrolyte at the interface resulting in the high degree of detachment of powder coating. The tape test on AA6060 after 1000 hours of AASS exposure confirmed intensive corrosion attack beneath the organic coating. The presence of corrosive species in combination with moisture leads to the chemical degradation of bonds at the interface, which resulted in the delamination of powder coating [46]. However, all oxide films generated at various vapour pressures of steam manifested that the steam generated oxide films provide good base for powder coating under various exposure conditions.

5 Conclusion

- Surface chemical composition analysis of the oxide film shows that notable amount of hydroxyl groups are present at the surface of oxide and verifies that the oxide film consists of boehmite.
- Electrochemical polarization measurements showed a reduction of anodic and cathodic activities up to 2 and 4 orders of magnitude respectively, while the treatment at high vapour pressure shifted the pitting potential to nobler values (+120 mV).
- Acetic acid salt spray and filiform corrosion results showed that corrosion resistance of steam generated oxide films with an industrial powder coating system was a function of vapour pressure of steam.
- The steam treatment of AA6060 with steam at vapour pressure of 1.9 bar resulted in superior powder coating adhesion in AASS and lowest length of filiform corrosion attack.
- Tape adhesion measurements showed that in wet environment steam generated oxide films at high vapour pressure showed improved adhesion properties. Although in dry condition the adhesion performance of these films was the same regardless of change in vapour pressure of steam.

Acknowledgments

The authors would like to thank Danish National Advanced Technology Foundation's financial support for the SIST project and all the involved project partners.

6 References

[1] M. Niknahad, S. Moradian, S.M. Mirabedini, The adhesion properties and corrosion performance of differently pretreated epoxy coatings on an aluminium alloy, Corros. Sci. 52 (2010) 1948–1957.

[2] S. Lin, H. Shih, F. Mansfeld, Corrosion protection of aluminum alloys and metal matrix composites by polymer coatings, Corros. Sci. 33 (1992) 1331–1349.

[3] W.S. Miller, L. Zhuang, J. Bottema, A.J. Wittebrood, P. De Smet, A. Haszler, et al., Recent development in aluminium alloys for the automotive industry, Mater. Sci. Eng. A. 280 (2000) 37–49.

[4] O. Engler, J. Hirsch, Texture control by thermomechanical processing of AA6xxx Al–Mg–Si sheet alloys for automotive applications—a review, Mater. Sci. Eng. A. 336 (2002) 249–262.

[5] G.E. Thompson, G.C. Wood, 5 - Anodic Films on Aluminium, in: J.C.S.B.T.-T. on M.S. and Technology (Ed.), Corros. Aqueous Process. Passiv. Film., Elsevier, 1983: pp. 205–329.

[6] G. Goeminne, H. Terryn, J. Vereecken, Characterisation of conversion layers on aluminium by means of electrochemical impedance spectroscopy, Electrochim. Acta. 40 (1995) 479–486.

[7] P. A. Sørensen, S. Kiil, K. Dam-Johansen, C.E. Weinell, Anticorrosive coatings: a review, J. Coatings Technol. Res. 6 (2009) 135–176.

[8] L.S.L. Anna L. Rowbotham Linda K. Shuker, Chromium in the environment: An evaluation of exposure of the UK general population and possible adverse health effects, J. Toxicol. Environ. Heal. Part B. 3 (2000) 145–178.

[9] J. Zhao, L. Xia, A. Sehgal, D. Lu, R.L. McCreery, G.S. Frankel, Effects of chromate and chromate conversion coatings on corrosion of aluminum alloy 2024-T3, Surf. Coatings Technol. 140 (2001) 51–57.

[10] P.D. Deck, D.W. Reichgott, Characterization of chromium-free no-rinse prepaint coatings on aluminum and galvanized steel, Met. Finish. 90 (1992) 29–35.

[11] M.A. Smit, J.M. Sykes, J.A. Hunter, J.D.B. Sharman, G.M. Scamans, Titanium based conversion coatings on aluminum alloy 3003, Surf. Eng. 15 (1999) 407–410.

[12] S.H. Wang, C.S. Liu, F.J. Shan, Corrosion behavior of a zirconium-titanium based phosphonic acid conversion coating on AA6061 aluminium alloy, Acta Metall. Sin. (English Lett. 21 (2008) 269–274.

[13] D. Zhao, J. Sun, L. Zhang, Y. Tan, J. Li, Corrosion behavior of rare earth cerium based conversion coating on aluminum alloy, J. Rare Earths. 28 (2010) 371–374.

[14] R.J. Racicot, R.L. Clark, H.-B. Liu, S.C. Yang, M.N. Alias, R. Brown, Anti-corrosion studies of novel conductive polymer coatings on aluminum alloys, in: Mater. Res. Soc. Symp. - Proc., 1996: pp. 529–534.

[15] C.-T. Lin, Green chemistry in situ phosphatizing coatings, Prog. Org. Coatings. 42 (2001) 226–235.

[16] I. Van Roy, H. Terryn, G. Goeminne, Study of the formation of zinc phosphate layers on AA5754 aluminium alloy, Trans. Inst. Met. Finish. 76 (1998) 19–23.

[17] J.W. Bibber, A Chrome-free conversion coating for aluminum with the corrosion resistance of chrome, Corros. Rev. 15 (1997) 303–313.

[18] M. Jariyaboon, P. Møller, R. Ambat, Effect of pressurized steam on AA1050 aluminium, Anti-Corrosion Methods Mater. 59 (2012) 103–109.

[19] D.G. Altenpohl, Use of Boehmite Films For Corrosion Protection of Aluminum, Corrosion. 18 (1962) 143t–153t.

[20] R.U. Din, M.S. Jellesen, R. Ambat, Characterization of Steam Generated Anticorrosive Oxide Films on Aluminium Alloys, Meet. Abstr. . MA2014-01 (2014) 471.

[21] R. Bainbridge, P. Lewis, J. Sykes, The effect of substrate preparation on the adhesion of polyethylene to aluminium, Int. J. Adhes. Adhes. 2 (1982) 175–179.

[22] M.P. Larsson, M.M. Ahmad, Improved polymer–glass adhesion through micro-mechanical interlocking, J. Micromechanics Microengineering. 16 (2006) S161–S168.

[23] W.P. Vellinga, G. Eising, F.M. de Wit, J.M.. Mol, H. Terryn, J.H.W. de Wit, et al., Adhesion at Al-hydroxide-polymer interfaces: Influence of chemistry and evidence for microscopic self-pinning, Mater. Sci. Eng. A. 527 (2010) 5637–5647.

[24] J. van den Brand, O. Blajiev, P.C.J. Beentjes, H. Terryn, J.H.W. de Wit, Interaction of ester functional groups with aluminum oxide surfaces studied using infrared reflection absorption spectroscopy., Langmuir. 20 (2004) 6318–26.

[25] A.N. Rider, The influence of porosity and morphology of hydrated oxide films on epoxy-aluminium bond durability, J. Adhes. Sci. Technol. 15 (2001) 395–422.

[26] A. Stralin, T. Hjertberg, Improved adhesion strength between aluminum and ethylene copolymers by hydration of aluminum surface, J. Appl. Polym. Sci. 49 (1993) 511–521.

[27] GSB international, International Quality Regulations For The Coating of Building Components, 2003.

[28] R. Perry, D. Green, Perry’s chemical engineers' handbook, McGraw-Hill, New York, 1997.

[29] V. 4. . NIST X-ray Photoelectron Spectroscopy Database, NIST X-ray Photoelectron Spectroscopy, (2012). http://srdata.nist.gov/xps/.

[30] J.T. Kloprogge, L. V Duong, B.J. Wood, R.L. Frost, XPS study of the major minerals in bauxite: gibbsite, bayerite and (pseudo-)boehmite., J. Colloid Interface Sci. 296 (2006) 572–6.

[31] J. Zähr, S. Oswald, M. Türpe, H.J. Ullrich, U. Füssel, Characterisation of oxide and hydroxide layers on technical aluminum materials using XPS, Vacuum. 86 (2012) 1216–1219.

[32] E. McCafferty, J.P. Wightman, Determination of the concentration of surface hydroxyl groups on metal oxide films by a quantitative XPS method, Surf. Interface Anal. 26 (1998) 549–564.

[33] T. Shih, P. Chen, Y. Huang, Effects of the hydrogen content on the development of anodic aluminum oxide film on pure aluminum, Thin Solid Films. 519 (2011) 7817–7825.

[34] M.R. Alexander, G.E. Thompson, G. Beamson, Characterization of the oxide/hydroxide surface of aluminium using x-ray photoelectron spectroscopy: a procedure for curve fitting the O 1s core level, Surf. Interface Anal. 29 (2000) 468–477.

[35] P. Centre, D.R. De Voreppe, F.- Voreppe, Acid-base properties of passive films on aluminum I. A photoelectrochemical study, J. Electrochem. Soc. 145 (1998).

[36] F. Cordier, E. Ollivier, X-ray Photoelectron Spectroscopy Study of Aluminium Surfaces Prepared by Anodizing Processes, 23 (1995) 601–608.

[37] Aerospace Industries Associaition, National Aerospace Standard (NAS) 1534, (1993). https://global.ihs.com/doc_detail.cfm?&rid=AIA&input_doc_number=1534&item_s_key=00079248&item_key_date=060816&input_doc_number=1534&input_doc_title=&org_code=AIA/NAS.

[38] R.U. Din, V. C. Gudla, M. S. Jellesen, R. Ambat, Accelerated growth of oxide film on aluminium alloys under steam: Part I: Synergetic effect of alloy chemistry and steam vapour pressure on microstructure., Unpubl. Work. (2014).

[39] J.P. Sargent, Adherend surface morphology and its influence on the peel strenght of adhesive joints bonded with modified phenolic and epoxy structural adhesives, Int. J. Adhes. Adhes. 14 (1994) 21–30.

[40] T. Semoto, Y. Tsuji, K. Yoshizawa, Molecular Understanding of the Adhesive Force between a Metal Oxide Surface and an Epoxy Resin, J. Phys. Chem. C. 115 (2011) 11701–11708.

[41] R. Ambat, A.J. Davenport, G.M. Scamans, A. Afseth, Effect of iron-containing intermetallic particles on the corrosion behaviour of aluminium, Corros. Sci. 48 (2006) 3455–3471.

[42] K. A. Yasakau, M.L. Zheludkevich, S. V. Lamaka, M.G.S. Ferreira, Role of intermetallic phases in localized corrosion of AA5083, Electrochim. Acta. 52 (2007) 7651–7659.

[43] J.D. Sinclair, J.E. Soc, Y. Martin, D. Abraham, H. Wickramasinghe, Corrosion Study of AA2024-T3 by Scanning Kelvin Probe Force Microscopy and In Situ Atomic Force Microscopy Scratching, J. Electrochem. Soc. 145 (1998) 2295–2306.

[44] P. Campestrini, E.P.M. van Westing, H.W. van Rooijen, J.H.W. de Wit, Relation between microstructural aspects of AA2024 and its corrosion behaviour investigated using AFM scanning potential technique, Corros. Sci. 42 (2000) 1853–1861..

[45] K. Nisancioglu, A. Afseth, G.M. Scamans, J.H. Nordlien, Influence of heat treatment and surface conditioning on filiform corrosion of aluminium alloys AA3005 and AA5754, Corros. Sci. 43 (2001) 2359–2377.

[46] K. Wapner, G. Grundmeier, Scanning Kelvin Probe Studies of Ion Transport and De-adhesion Processes at Polymer/Metal Interfaces, Adhes. Curr. Res. Appl. (2006) 507–524.

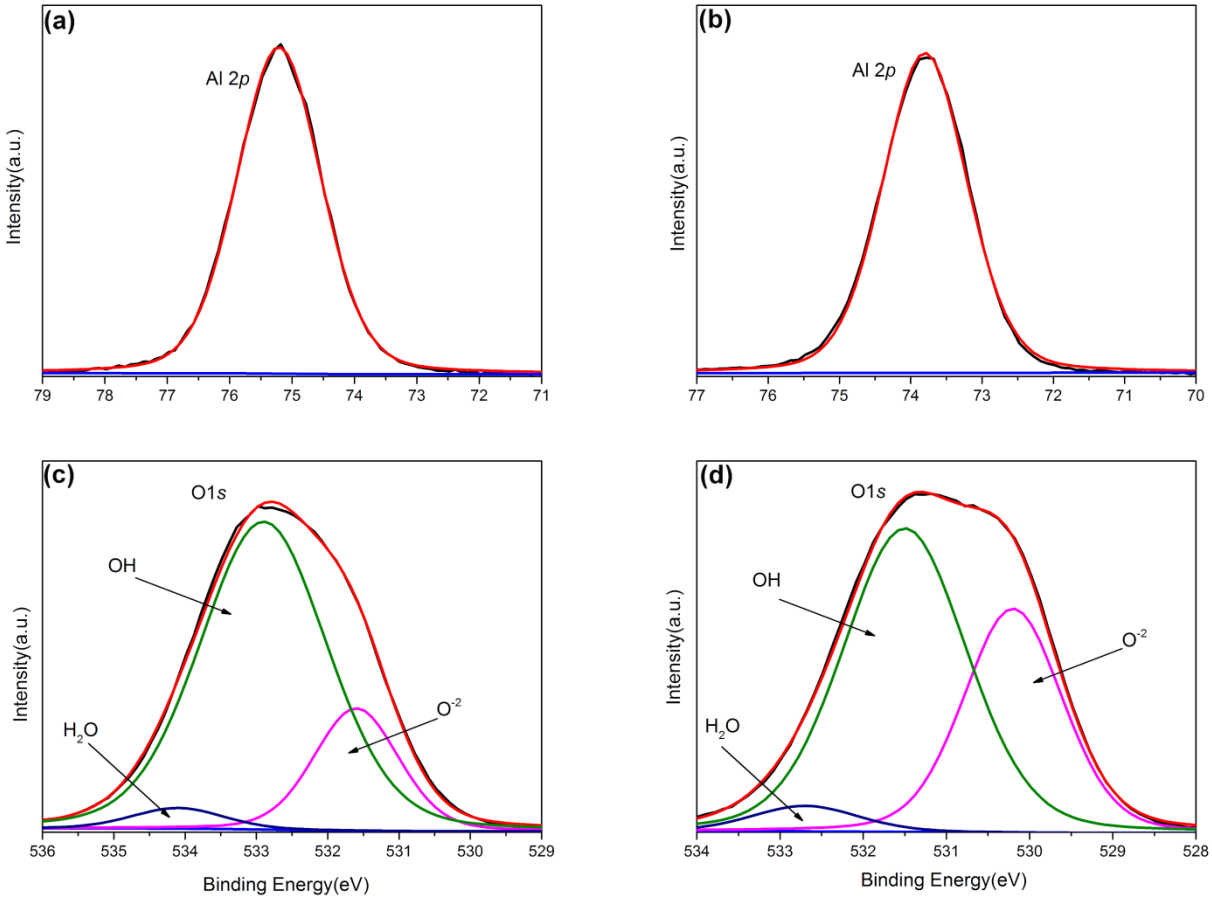

Figure 1

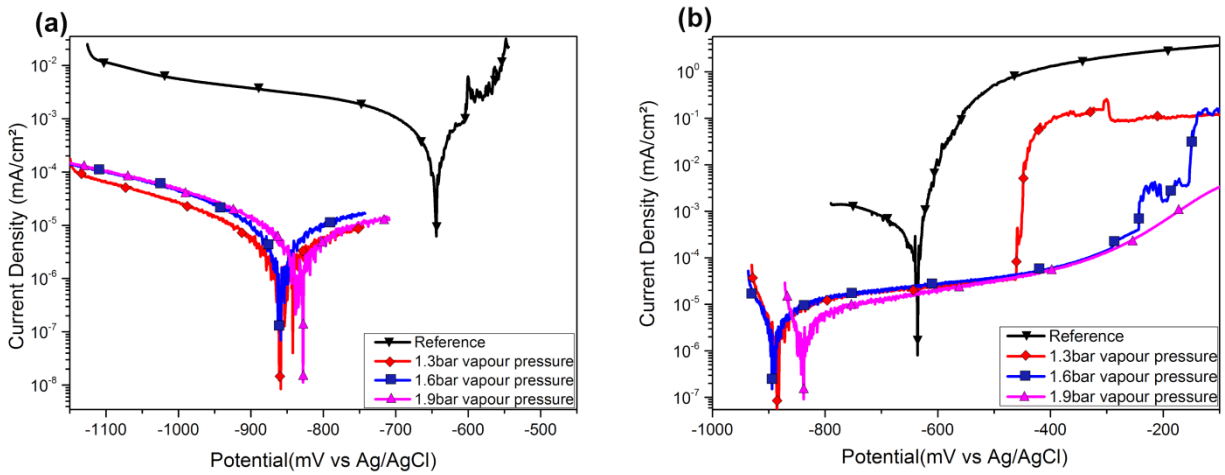

Figure 2

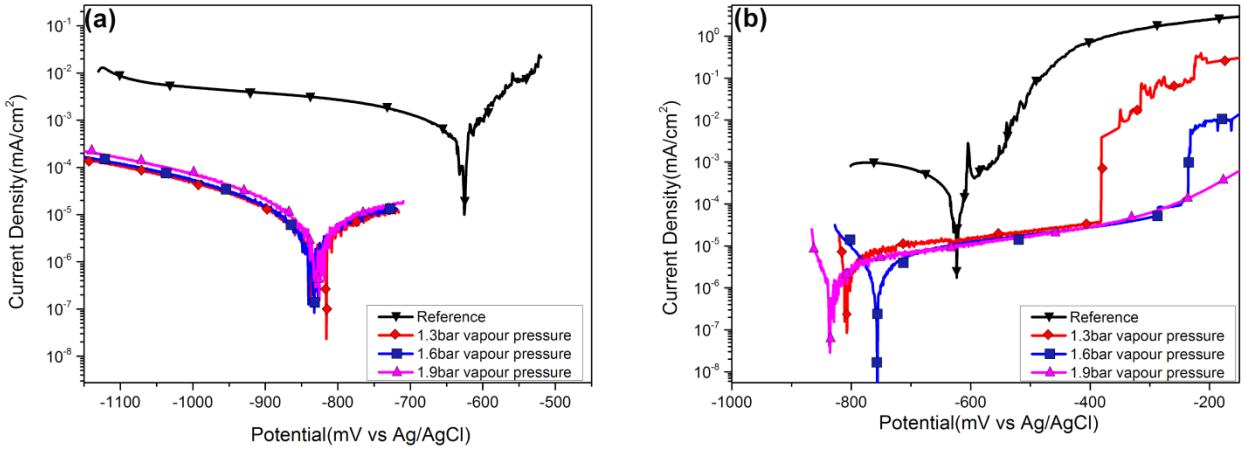

Figure 3

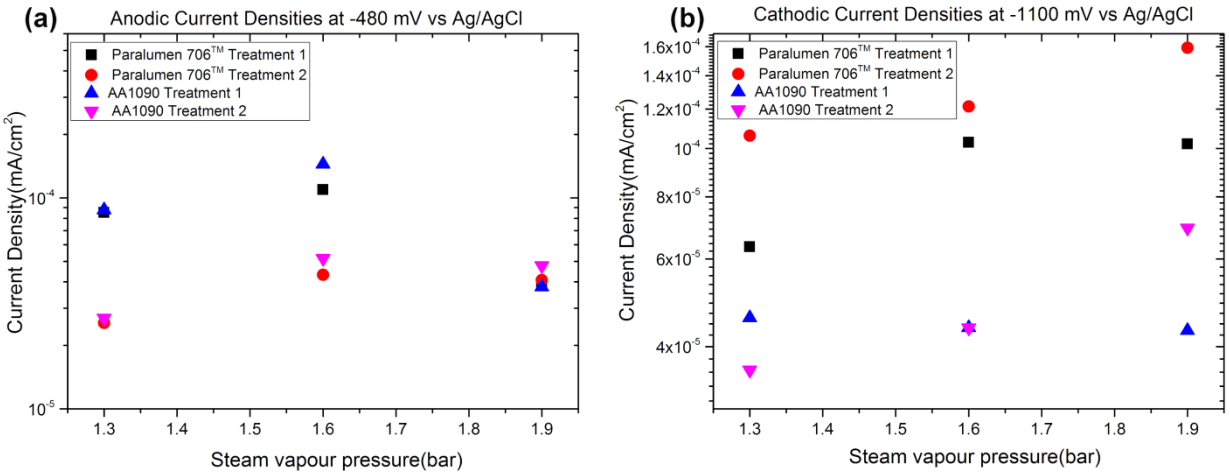

Figure 4

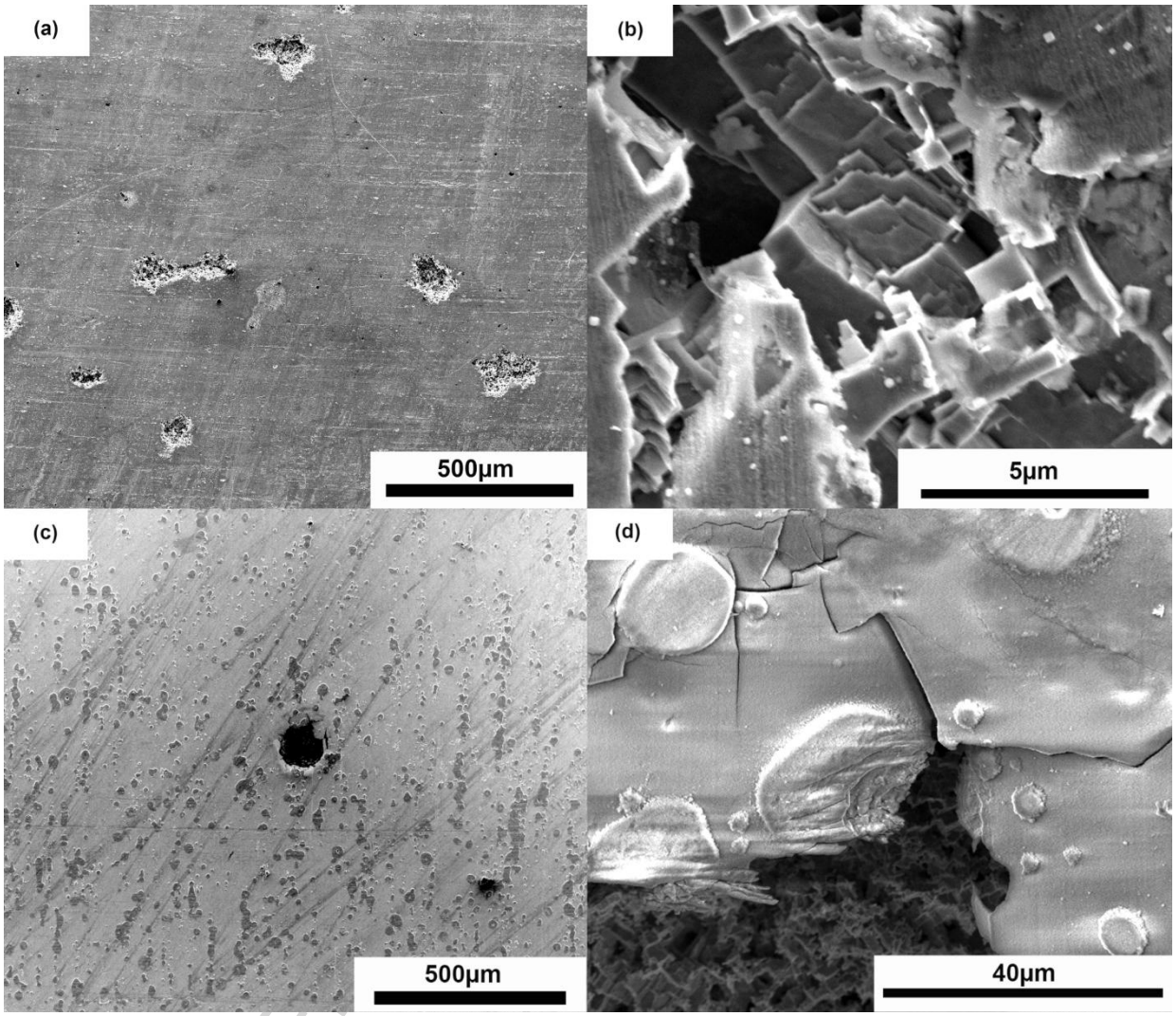

Figure 5

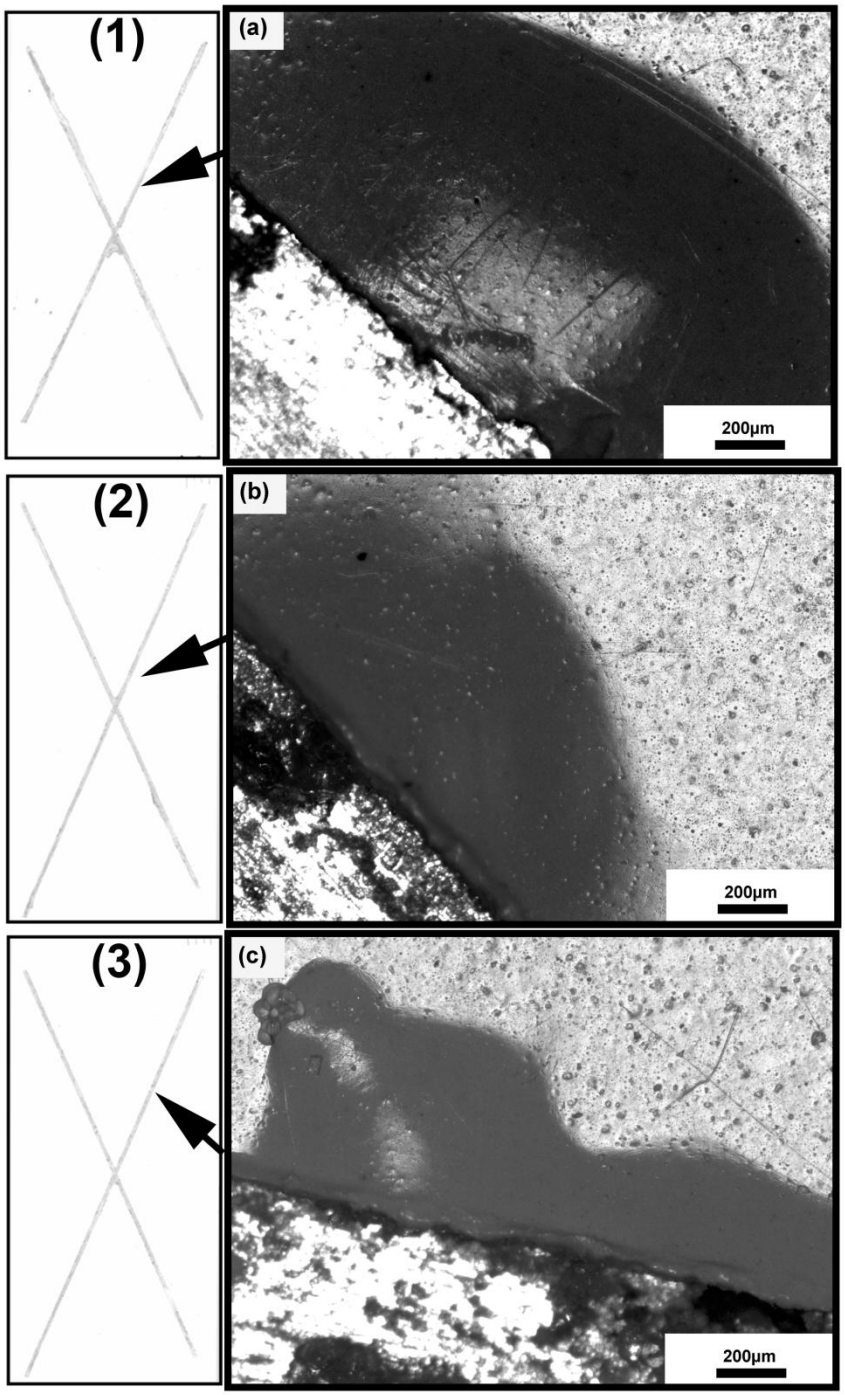

Figure 6

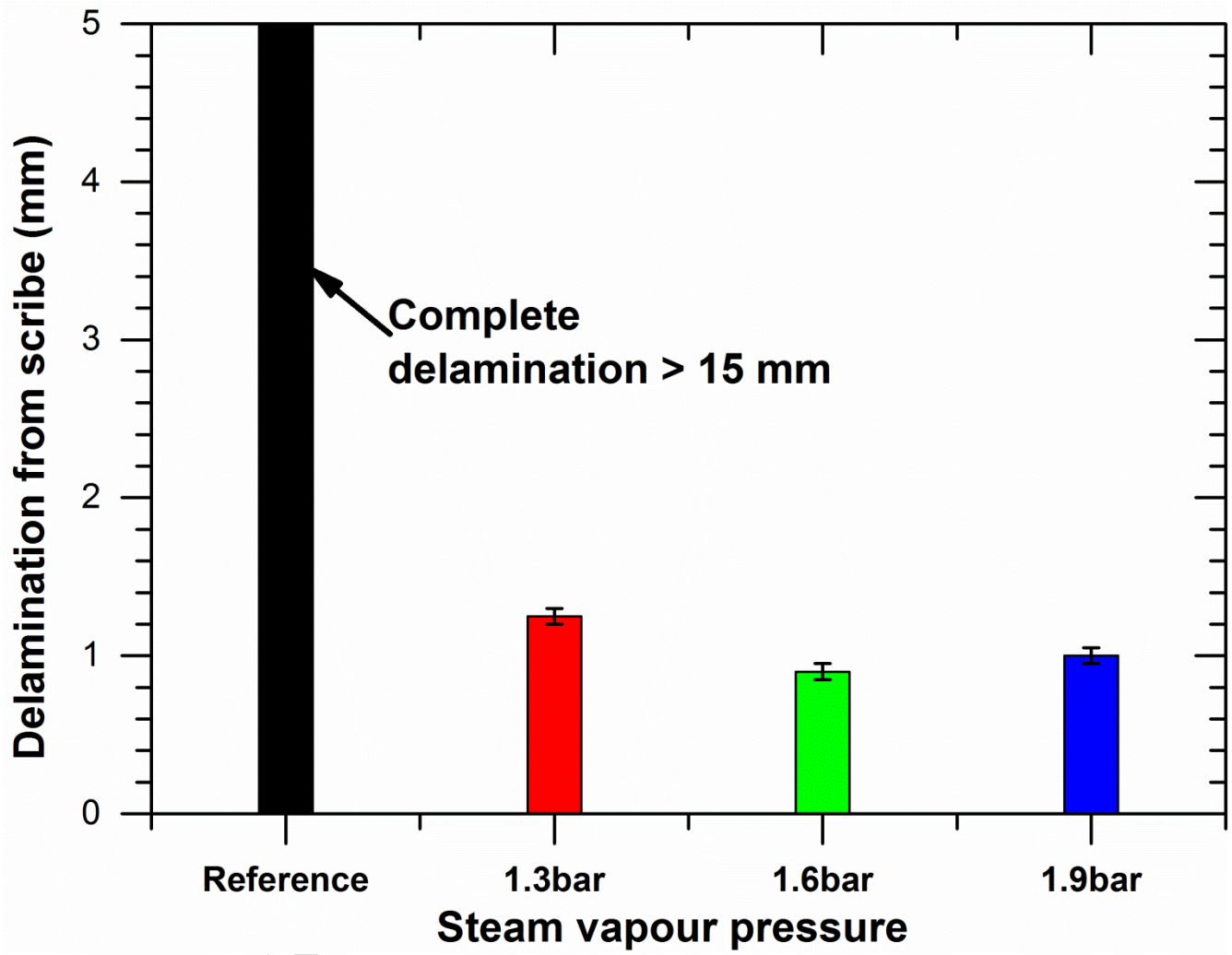

Figure 7

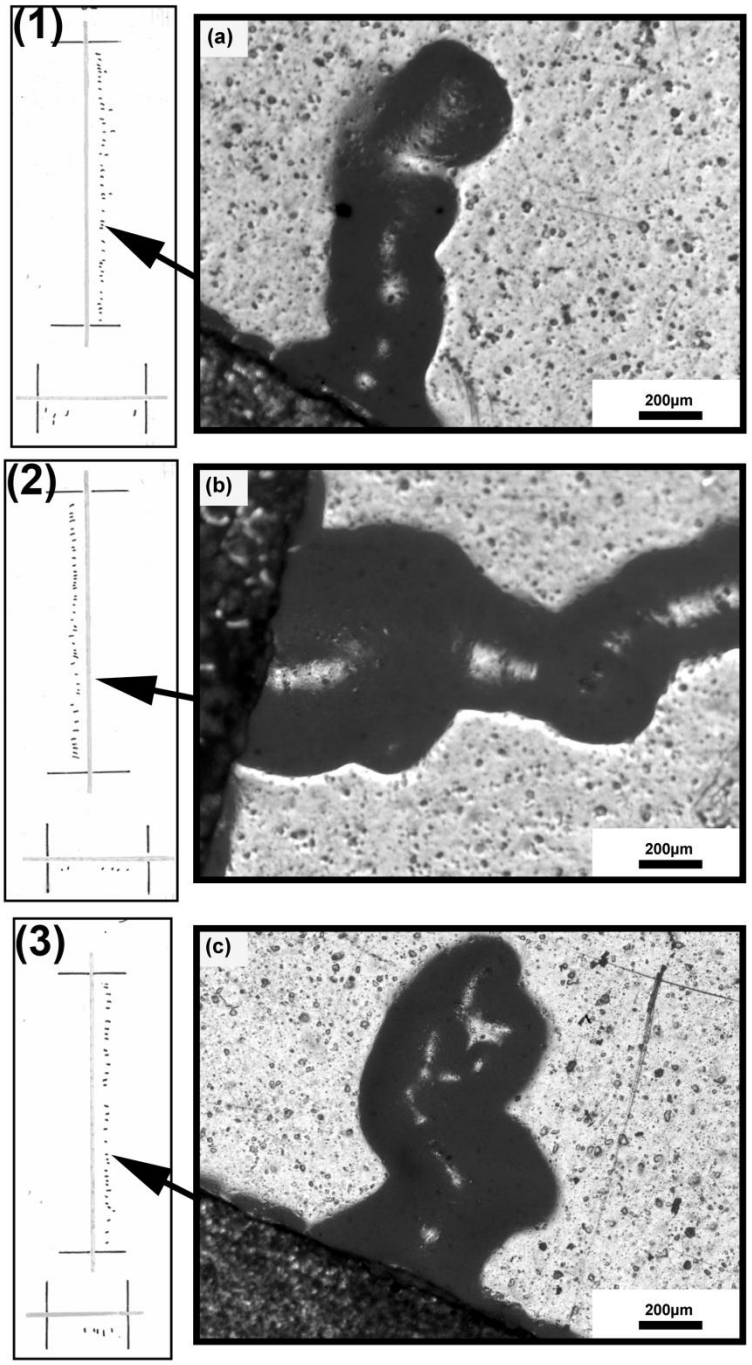

Figure 8

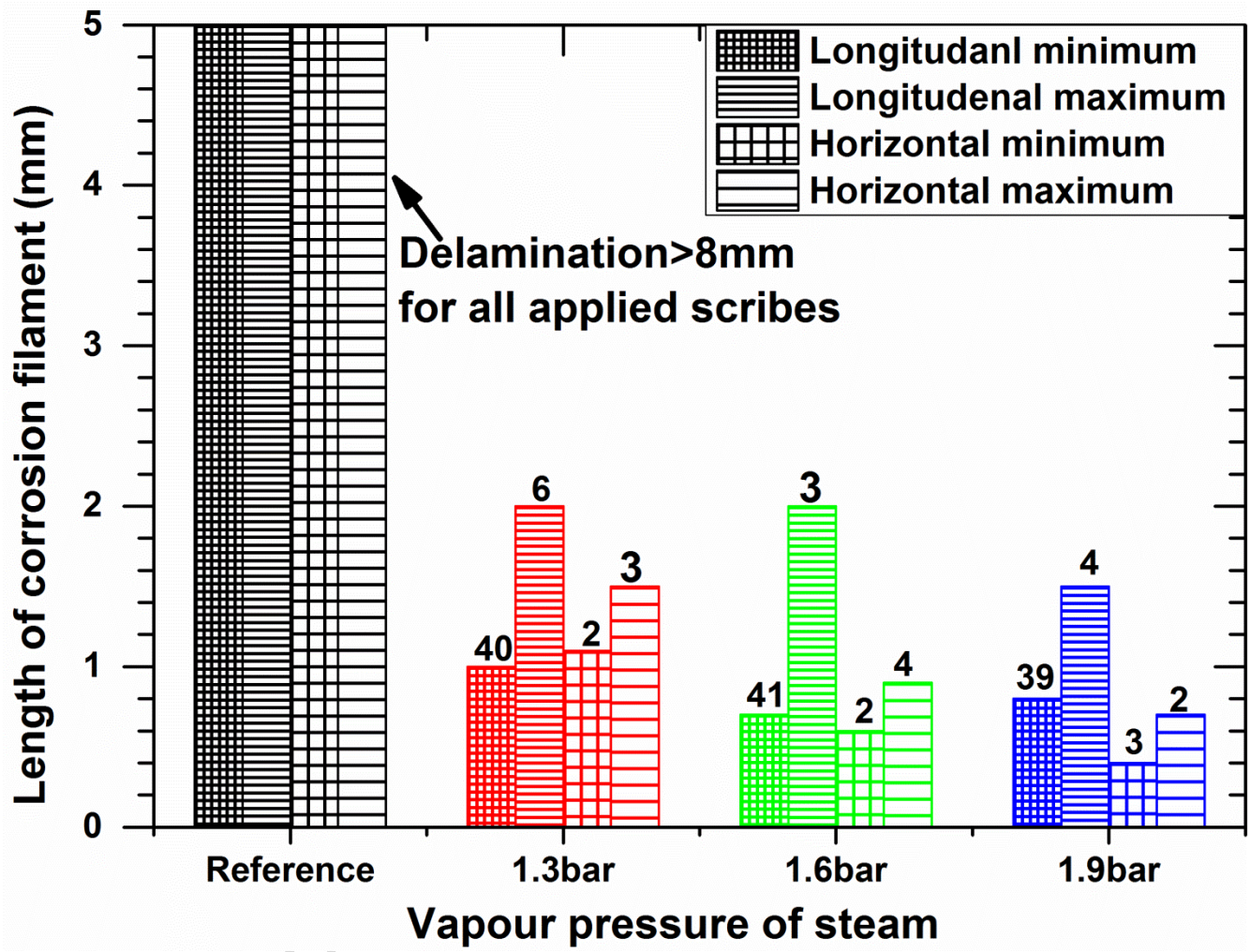

Figure 9

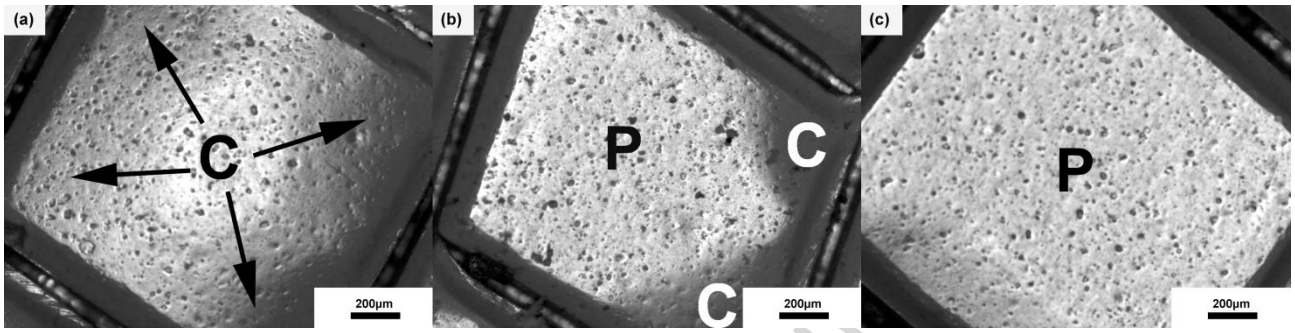

Figure 10

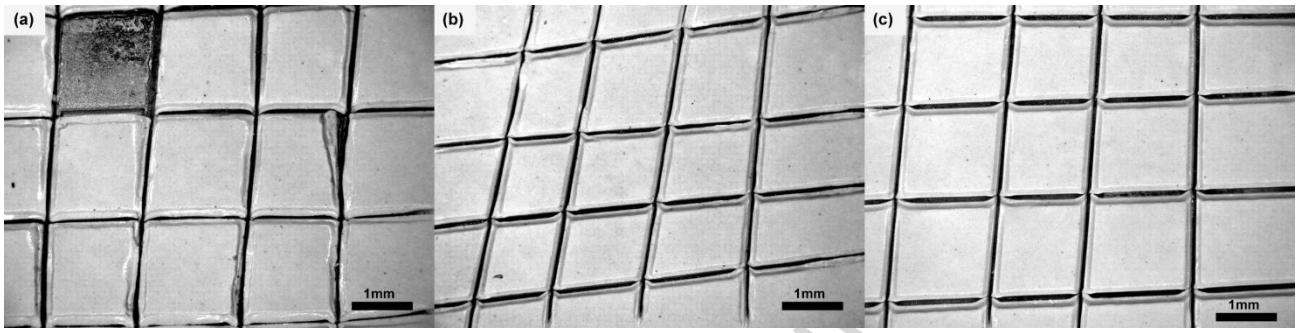

Figure 11

Table I Chemical composition of AA6060 in weight %, remainder Al.

Si	Fe	Cu	Mn	Mg	Cr	Zn	Ti
0.3-0.6	0.1-0.3	max. 0.1	max. 0.1	0.3-0.6	0.05	0.1	0.1

Table II Breakdown anodic potential (-950 mV to -100 mV) of steam generated oxide films at different vapour pressure of steam.

Sample	1.3 bar	1.6 bar	1.9 bar
AA1090-Treatment 1	≥-405 mV	No failure	No failure
AA1090-Treatment 2	≥-210 mV	No failure	No failure
Peraluman 706™ -Treatment 1	≥-460 mV	≥-290 mV	No failure
Peraluman 706™ -Treatment 2	≥-380 mV	≥-230 mV	No failure

List of figure captions

Figure 1 XPS spectra of the Al 2*p* and O 1*s* levels for the surface of AA1090 samples treated by steam for 30 s (a, c) and 10 min. (b, d) at 1.3 bar vapour pressure.

Figure 2 Cathodic (a) and anodic (b) Potentiodynamic polarization curves for Peraluman 706™ (treatment process 1) in naturally aerated 0.1M NaCl solution before and after exposure to the steam of different vapour pressure for 10 min.

Figure 3 Cathodic (a) and anodic (b) Potentiodynamic polarization curves for Peraluman 706™ (treatment process 2) in naturally aerated 0.1M NaCl solution before and after exposure to the steam of various vapour pressure for 10 min.

Figure 4 Measured anodic and cathodic current densities at -480 mV (a) and -1100 mV (b) of AA1090 and Peraluman 706™ samples treated with steam having different vapour pressure, for 10 minutes.

Figure 5 Surface morphology after anodic polarization: (a) Peraluman 706™ after treatment 1, (c) surface of Peraluman 706™ treated with steam having vapour pressure of 1.3 bar, for 10 minutes. (b), (d) are high magnification images of pit in (a) and (c), respectively.

Figure 6 The overview of scribed area of sample and local detachment of powder coating on AA6060 steam treated samples with (1), (a) 1.3 bar, (2), (b) 1.6 bar and (3), (c) 1.9 bar steam vapour pressure after 1000 hours of AASS test.

Figure 7 Average length of powder coating delamination on reference AA6060 steam, treated samples with 1.3 bar , 1.6 bar and 1.9 bar steam vapour pressure after 1000 hours of AASS test.

Figure 8 Growth of filiform corrosion filament after 1000 hrs of FFC test on steam treated and powder coated AA6060 surface, with (a) 1.3 bar, (b) 1.6 bar and (c) 1.9 bar steam vapour pressure, while (1), (2), and (3) shows the scribed samples after the filiform corrosion test of steam treated AA6060 at 1.3 bar, 1.6 bar and 1.9 bar, respectively.

Figure 9 Length of filiform corrosion filament after 1000 hours of FFC test of reference and steam treated and powder coated AA6060 surface, with (a) 1.3 bar, (b) 1.6 bar and (c) 1.9 bar steam pressure and total number of filaments are presented at the top of each bar.

Figure 10 Optical micrographs of individual squares in powder coated areas of the grid on the specimen treated with (a) 1.3 bar, (b) 1.6 bar, and (c) 1.9 bar steam vapour pressure, after exposure to 1000 h of AASS test. The intact areas of powder coating have been marked as "P" whereas detached areas of powder coating are marked as "C", respectively.

Figure 11 Cross cut areas of the specimen treated with (a) 1.3 bar, (b) 1.6 bar, and (c) 1.9 bar steam vapour pressure, exposed to 1000 hours of AASS and subjected to tape test.

Highlights to manuscript

Accelerated growth of oxide film on aluminium alloys under steam: Part II: Synergetic effect of alloy chemistry and steam vapour pressure on corrosion performance.

by Rameez Ud Din, Kirill Bordo, Morten S. Jellesen, Rajan Ambat

- The formation of boehmite film on aluminium alloys surface.
- Boehmite enhanced corrosion resistance properties of the metal substrate.
- The pitting potential was a function of the vapour pressure of the steam.
- Filiform and acid salt spray performance was related to steam vapour pressure.